Memoirs of the Faculty of Engineering, Nagoya University
Vol. 34, No. 1 (1982) — Research Report —

A STUDY ON THE FLUCTUATION CONCENTRATION FIELD IN A TURBULENT JET

——On the Measurement of the Concentration Fluctuation Intensity and the Self-Preservation——

IKUO NAKAMURA and YASUHIKO SAKAI

Department of Mechanical Engineering

MASAFUMI MIYATA

Department of Mechanical Engineering, Yamanasi University

(Received May 26, 1982)

Abstract

In this report, presented are the experimental results of the diffusion process in a circular jet of a dye solution issuing into a quiescent water. Also a semi-empirical theory for the radial profile of the concentration fluctuation intensity is presented. Measurements of the concentration field for a dye solution were performed by a light absorption method because of the simplicity of its measuring principle and movability of the probe.

Experimental results showed that the radial profiles of the mean axial velocity and mean concentration had well-known Gaussian distributions respectively. A self-preserving form for the profiles of the concentration fluctuation intensity was observed in the downstream region, $x/d_N \geq 100$. Using these experimental results and assumtions of the gradient type diffusion process, an analysis and calculations are presented on the self-preserving profile of the concentration fluctuation intensity.

1. Introduction

The diffusivity of turbulence is one of the most important characteristics of turbulent flows. Investigation of the turbulent diffusion is essential to understand

the mechanism of turbulence and also necessary from an engineering point of view. For instance, in order to mix the various liquids effectively in chemical engineering and to predict the air pollution or ocean pollution which are most serious in the public nuisance problems, an accumulation of fundamental knowledge about the turbulent diffusion is indispensable. For those purposes, it is insufficient only to measure the average concentration of diffusion matter so the detection of concentration fluctuations becomes important.

Up to now, as the methods to measure the concentration fluctuations the conductivity probe method, light-scattering method, light-absorption method and laser Raman- scattering method, etc. have been tried but the most effectual method has not yet been established. In this study, a light-absorption method[3] is adopted, mainly in consideration of the simplicity of the measuring principle and movability of the probe. As a first stage of the study on the turbulent diffusion by using this concentration fluctuation measuring system, a circular free jet which is one of the most fundamental flows is surveyed. Although on the study of turbulent diffusion of a scalar quantity for this case many papers[4~8] have been published because of its simplicity of the flow configuration, it seems that the measurement of the jet diffusion by the light-absorption method has not yet been reported.

Therefore, in this study firstly the mean concentration field, fluctuating concentration field for a circular free jet were measured by the light-absorption method to far downstream region (up to $300d_N$) from the nozzle exit and in the region $x/d_N \geq 100$ the existence of self-preservation for the concentration field was confirmed.

Next, on a radial profile of the concentration fluctuation intensity, the self-preserving solution is calculated by using the gradient type model for the diffusion process and its properties are investigated. On the basis of the experimental data, the balances of the concentration fluctuation intensity are also studied and the propriety of the gradient type diffusion model is discussed.

Nomenclature

x, y, z, r = axial, horisontal, vertical and radial coordinates respectively (see Fig. 3)

U_x, U_r, Γ, P = mean axial velocity, mean radial velocity, mean concentration and mean pressure respectively

u_x, u_r, γ, p = fluctuation values for axial velocity, radial velocity, concentration and pressure respectively

$\boldsymbol{U}$, $\boldsymbol{u}$ = mean velocity vector and velocity fluctuation vector respectively

a_1, a_2, a_3 = x coordinates of virtual origins for mean axial velocity, mean concentration and concentration fluctuation intensity respectively

η_1, η_2, η_3 = non-dimensional radial coordinates, they are defined by

$$\eta_1=\frac{r}{x-a_1},\quad \eta_2=\frac{r}{x-a_2} \text{ and } \eta_3=\frac{r}{x-a_3}$$

respectively

d_N = nozzle diameter

D_m = molecular diffusivity of matter

ν = kinematic viscosity of water
χ = dissipation rate of the concentration fluctuation
$\chi=2D_m\overline{(\text{grad}\,\gamma)\cdot(\text{grad}\,\gamma)}$
a = x coordinate of the virtual origin for the self-preserving function
α = a/d_N
ξ, η = self-preserving axial and radial coordinates, they are defined by $\xi=x/d_N$ and $\eta=\dfrac{r}{x-a}=\dfrac{r}{d_N(\xi-\alpha)}$ respectively
λ_T = dissipation length scale for the concentration fluctuations
ν_T = eddy viscosity
D_T = eddy diffusivity
$\overline{\ }$ = time averaged value
$\sim$ = instanteneous value
$'$ = root-mean-square value

subscripts
c = value on the jet axis
j = value at the exit of the nozzle

2. Measuring System and Experimental Apparatus

Fig. 1 shows a whole diagram of the measuring system. The light emitted from the tungsten lamp is introduced into the test section by the light guide after passing through the lense system and the optical filter. The intensity of the light introduced into the test section attenuates strictly according to Lambert-Beer's absorption law[1~3] for each wavelength component due to an action of the light absorptive matter. The modified light which has received the informations of the concentration fluctuations at the test section passes again through the light guide and then by the lense system it is focused on the cathode surface of the photomultiplier. We can finally detect the photomultiplier's voltage output $\tilde{E}_p$ which is proportional to the light intensity. In this case, it shoud be noticed that the deviation from Lambert-Beer's law in a relation between the photomultiplier's output $\tilde{E}_p$ and the concentration $\tilde{\Gamma}$ of the light absorptive matter may be observed apparently, because of a broad band spectral distribution of the light source and various spectral characteristics of each optical element in the measuring system. However, when we will detect the concentration practically, it is desirable that the $\tilde{E}_p\sim\tilde{\Gamma}$ relation follows on a simple power law such as Lambert-Beer's law and for such practical purposes matching of optical characteristics for each optical element in the measuring system becomes important. (see ref. (3) in detail)

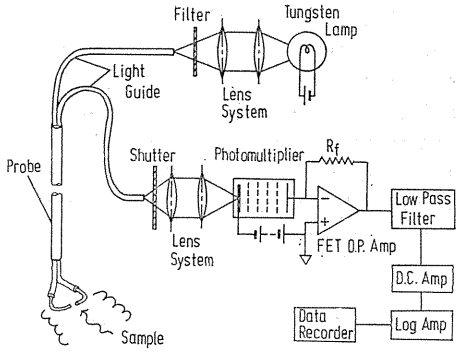

Fig. 1. The whole diagram of the measuring system.

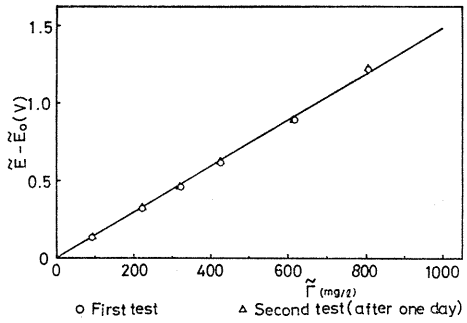

Fig. 2. Output $\tilde{E}$ of the logarithmic ampifier vs concentration $\tilde{\Gamma}$.

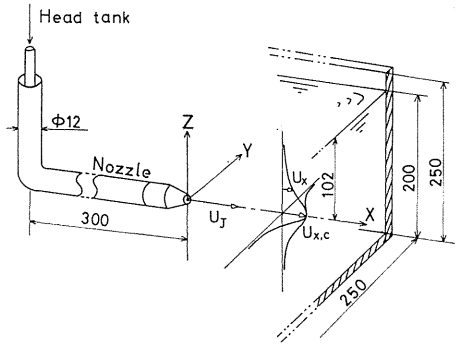

Fig. 3. The coordinate system and the working section.

In this measuring system, BPB-50 (Fuji Film Inc.) as an optical filter was used and the water solution of D. F. Orange (direct dye) as the light absorptive matter, optical glass fibers (fiber's bundle diameter $d_f=0.5$mm) as light guides were used. A sample volume of the test section in this case was about 1.4×10^{-4}cc. By using this measuring system, we could make the $\tilde{E}_p\sim\tilde{\Gamma}$ relation obey to a simple power law quite well and consequently the relation between the final output $\tilde{E}$ linearized by the logarithmic O. P. amplifier and the concentration $\tilde{\Gamma}$ showed a linearity sufficient to detect the concentration fluctuations. (see Fig. 2)

Fig. 3 shows a sketch of the coordinate system and a working section. The flow system consisted of a free dyed water jet issuing from a nozzle which has an exit diameter d_N of about 1.02mm and the Reynolds number $Red_N=U_Jd_N/\nu$ was adjusted to about 5000. To measure the mean axial velocity U_x, a laser doppler anemometer (which will be abbriviated to LDV hereafter) and the pitot tube with an inner diameter of 0.4mm and an outer diameter of 0.73mm were both used, while Y.H.P's r.m.s. voltage meter was used to measure r.m.s. values of the concentration fluctuations.

3. Experimental Results and Discussion

3. 1. Velocity field

In this section, the results for the velocity field of the jet which will give fundamental knowledge to the later consideration for the self-preservation of the concentration field will be presented.

Fig. 4 shows radial profiles of the non-dimensional mean axial velocity $U_x/U_{x,c}$ measured by LDV at x-z cross sections of various axial locations, where $U_{x,c}$ is the mean axial velocity on the jet axis. It can be seen that the profiles have a similar shape in the pretty wide extent

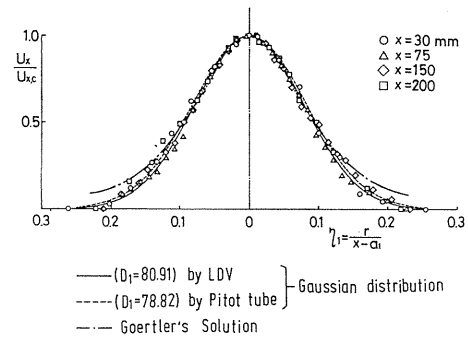

Fig. 4. The radial profiles of the mean axial velocity.

$30 \leq x/d_N \leq 200$. These radial profiles can be accurately described in terms of the following Gaussian function:

$$U_x/U_{x,c} = \exp(-D_1\eta_1^2) \tag{1}$$

where $\eta_1 = r/(x-a_1)$, D_1 = constant. In Fig. 4, the solid line represents the Gaussian profile with $D_1 = 80.91$, $a_1 = -2.79d_N$ and the broken line shows the Gaussian profile with $D_1 = 73.82$, $a_1 = 5.93d_N$ which was obtained from the measurements by the pitot tube. Both Gaussian profiles are in good agreement with each other. The chain line is Goertler type's solution in terms of the following function:

$$U_x/U_{x,c} = (1+K\eta_1^2)^{-2} \tag{2}$$

where $K = U_{x,c}(x-a_1)/8\nu_T$, $a_1 = 5.93d_N$. The line shown in Fig. 4 is a profile with $K = 45.91$.

Fig. 5 shows the radial profiles of the non-dimensional eddy viscosity $\nu_T/U_{x,c}(x-a_1)$, which were calculated from the Goertler type's profile (2) by using the measured values by the pitot tube for both x–z cross sections and x–y cross sections. The solid lines in Fig. 5 show the average values for x–z cross sections and x–y cross sections, being 0.00264 and 0.00280 respectively. The Goertler type's profile in Fig. 4 (a chain line) is the one with an average value 0.00272 of above two values for each cross section.

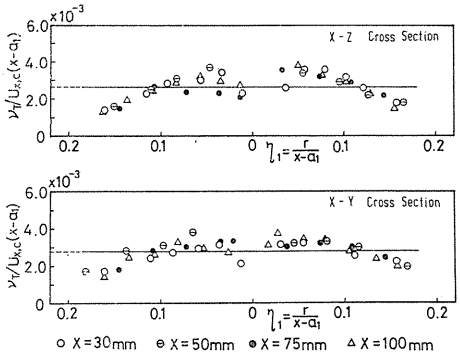

Fig. 5. The radial profiles of eddy viscosity ν_T computed from the Goertler type's solution.

3. 2. *Concentration field*

The non-dimensional mean concentration profiles Γ/Γ_C for x–z cross sections are shown in Fig. 6. Although there exist a scattering of measured values in the outer region of the jet, it can be seen that in the extent $50 \leq x/d_N \leq 175$ the profiles have a similar shape which can be described in terms of the following Gaussian function:

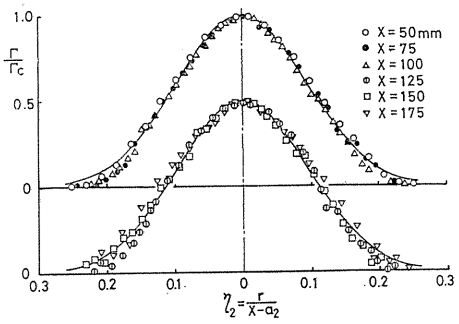

Fig. 6. The radial profiles of the mean concentration.

$$\Gamma/\Gamma_c = \exp(-D_2\eta_2^2) \tag{3}$$

where $\eta_2 = r/(x-a_2)$, D_2 = constant. The solid line in Fig. 6 represents a Gaussian profile with $D_2 = 53.3$, $a_2 = 4.37d_N$.

Fig. 7 shows a radial distribution curve of the turbulent Schmidt number $S_{CT} = \nu_T/D_T$, which was calculated by integrating the mean velocity Eq. (5b) and mean

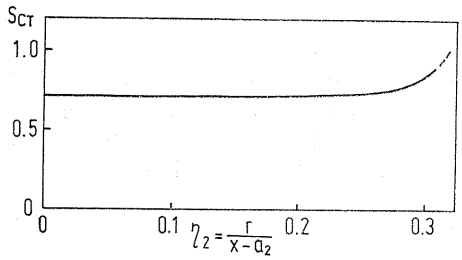

Fig. 7. The radial profile of turbulent Schmidt number S_{CT}.

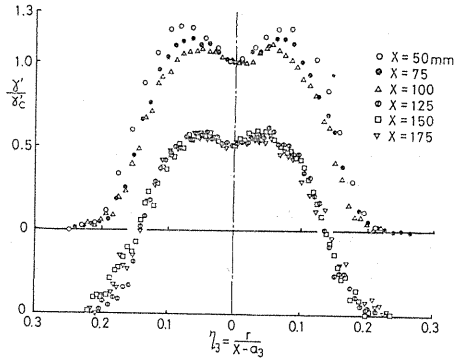

Fig. 8. The radial profiles of the concentration fluctuation r.m.s. value γ'.

concentration Eq. (5c) which will be given in the next chapter on the assumption that the radial profiles of the mean velocity and mean concentration can be approximated to Gaussian curves (1), (3) respectively. As shown in Fig. 7, S_{CT} has an almost constant value, which is about 0.712, across the entire jet width.

In Fig. 8, shown are the radial profiles of the non-dimensional concentration fluctuation r.m.s. values γ'/γ_C' obtained by processing the data by means of Y.H.P.'s r.m.s. voltage meter, where γ_C' is the r.m.s. value on the jet axis and the radial displacement is normalized by the distance $x-a_3$ from the virtual origin for γ_C', a_3 being $-4.07d_N$. As shown in this figure, the profiles of γ'/γ_C' have a remarkable change in the relatively near region from the nozzle $50 \leq x/d_N \leq 100$ and only in pretty downstream extent $100 \leq x/d_N$ profiles become similar. It should be here noticed that the signals of concentration fluctuations contain rather low frequency components (10~30Hz) so it is infered that there exist appreciable error in the values of γ' obtained by using Y.H.P.'s r.m.s. voltage meter. However, it can be considered that qualitatively the properties such as a remarkable change of γ' profiles in the near region from the nozzle exit and the existence of a similar shape in $100 \leq x/d_N$ may be correct.

The axial profile of the relative intensity γ_C'/Γ_C of the concentration fluctuation r.m.s. value γ_C' to the mean concentration Γ_C is shown in Fig. 9. It can be seen from this figure that, after the rapid increase of γ_C'/Γ_C in the near region from the nozzle, a gradual increase continues and γ_C'/Γ_C approaches an asymptotic value 20.9% in $x/d_N \geq 100$.

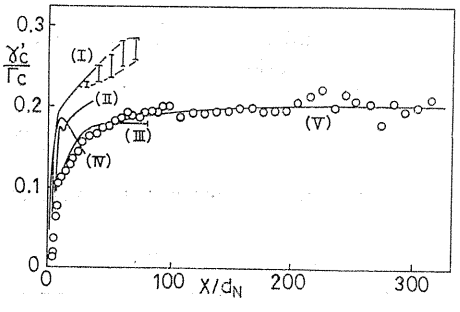

Fig. 9. The axial profile of the relative intensity γ_C'/Γ_C on the jet axis.
○ Present work; (Ⅰ) Birch et al.[5], free methane jet; (Ⅱ) Becker et al.[4], concentration (air jet); (Ⅲ) Wilson & Dankwerts[8], temperature; (Ⅳ) Corrsin & Uberoi[7], temperature; (Ⅴ) Present similar distribution.

4. Self-Preserving Solution for the $\overline{\gamma}^2$-equation

4. 1. Fundamental equations

As the self-preservation for the $\overline{\gamma}^2$ distributions can be observed apparently in the experimental results, in this chapter the self-preserving solution will be pursued. The fundamental equations are described in the vector form as follows:

$$\mathrm{div}\,\boldsymbol{U}=0 \qquad \text{continuity Eq.} \qquad (4a)$$

$$\mathrm{div}\,(\boldsymbol{U}\circ\boldsymbol{U}+\overline{\boldsymbol{u}\circ\boldsymbol{u}})=-\frac{1}{\rho}\,\mathrm{grad}\,P+\nu\nabla^2\boldsymbol{U} \qquad \text{mean velocity Eq.} \qquad (4b)$$

$$\mathrm{div}\,(\boldsymbol{U}\Gamma+\overline{\boldsymbol{u}\cdot\gamma})=D_m\nabla^2\Gamma \qquad \text{mean concentration Eq.} \qquad (4c)$$

$$\mathrm{div}\,(\boldsymbol{U}\overline{\gamma}^2)+2\overline{\gamma\boldsymbol{u}}\cdot\mathrm{grad}\,\Gamma+\mathrm{div}\,(\overline{\boldsymbol{u}\gamma}^2)$$
$$=D_m\nabla^2\overline{\gamma}^2-2D_m\overline{(\mathrm{grad}\,\gamma)\cdot(\mathrm{grad}\,\gamma)} \qquad \overline{\gamma}^2 \text{ Eq.} \qquad (4d)$$

With the thin-shear-layer approximation, in terms of vector components the above equations (4a, b, c, d) reduce to

$$\frac{\partial U_x}{\partial x}+\frac{1}{r}\frac{\partial}{\partial r}(uU_r)=0 \qquad \text{continuity Eq.} \qquad (5a)$$

$$U_x\frac{\partial U_x}{\partial x}+U_r\frac{\partial U_x}{\partial r}=\frac{1}{r}\frac{\partial}{\partial r}\{r(-\overline{u_xu_r})\} \qquad \text{mean velocity Eq.} \qquad (5b)$$

$$U_x\frac{\partial\Gamma}{\partial x}+U_r\frac{\partial\Gamma}{\partial r}=\frac{1}{r}\frac{\partial}{\partial r}\{r(-\overline{\gamma u_r})\} \qquad \text{mean concentration Eq.} \qquad (5c)$$

$$U_x\frac{\partial\overline{\gamma}^2}{\partial x}+U_r\frac{\partial\overline{\gamma}^2}{\partial r}+2\overline{\gamma u_r}\frac{\partial\overline{\gamma}^2}{\partial r}+\frac{1}{r}\frac{\partial}{\partial r}(r\overline{\gamma^2u_r})+\chi=0$$

advection by U_x — advection by U_r — production — diffusion — dissipation

$$\overline{\gamma}^2 \text{ Eq.} \qquad (5d)$$

where $\chi=2D_m\overline{(\mathrm{grad}\,\gamma)\cdot(\mathrm{grad}\,\gamma)}$. In this stage, the following assumptions will be made.

1) Assumptions of the gradient type diffusion process; they are

$$-\overline{u_xu_r}=\nu_T\frac{\partial U_x}{\partial r} \qquad (6), \qquad -\overline{\gamma u_r}=D_T\frac{\partial\Gamma}{\partial r} \qquad (7)$$

$$-\overline{\gamma^2u_r}=\frac{\nu_T}{\sigma_{\gamma^2}}\frac{\partial\overline{\gamma}^2}{\partial r} \qquad (8)$$ [9)]

where ν_T is eddy viscosity, D_T is turbulent diffusivity and σ_{γ^2} is the quantity correspond to turbulent Schmidt number for the concentration fluctuation intensity respectively.

2) Self-preserving coordinates are defined by

$$\xi=x/d_N, \quad \eta=r/(x-a)=r/\{d_N(\xi-\alpha)\}$$

where a is x coordinate of the virtual origin and α equals a/d_N.

3) Assumptions of an isotropic field for the dissipation term; they are

$$\chi=2D_m\overline{(\mathrm{grad}\,\gamma)\cdot(\mathrm{grad}\,\gamma)}=12D_m\bar{\gamma}^2/\lambda_\gamma^2 \quad [10] \tag{9}$$

$$\lambda_\gamma=\varepsilon(x-a)=\varepsilon d_N(\xi-\alpha) \quad [11\sim14] \tag{10}$$

where λ_γ is the dissipation length scale for the concentration fluctuations and ε is a constant which is the function of Re_{dN} in general.

In order to obtain self-preserving solutions by using these assumptions, we put

$$f_1(\eta)=U_x/U_{x,c}, \quad f_2(\eta)=\frac{df_1}{d\eta}, \quad f_3(\eta)=U_r/U_{x,c}$$

$$f_4(\eta)=\Gamma/\Gamma_c, \qquad f_5(\eta)=\frac{df_4}{d\eta}, \quad f_6(\eta)=\bar{\gamma}^2/\bar{\gamma}^2_c$$

where the subscript c shows the value on the jet axis. With the assumptions 1)$\sim$3) and definitions given above, the equations (5a, b, c, d) read

$$\frac{d}{d\eta}(\eta f_1)-\frac{1}{\eta}\frac{d}{d\eta}(\eta f_3)=0 \qquad \text{continuity Eq.} \tag{11a}$$

$$\frac{df_1}{d\eta}(f_3-\eta f_1)-f_1^2=\frac{1}{\eta}\frac{d}{d\eta}\left(B(\eta)\eta\frac{df_1}{d\eta}\right) \qquad \text{mean velocity Eq.} \tag{11b}$$

$$\frac{df_4}{d\eta}(f_3-\eta f_1)-f_1f_4=\frac{1}{\eta}\frac{d}{d\eta}\left(D(\eta)\eta\frac{df_4}{d\eta}\right) \quad \text{mean concentration Eq.} \tag{11c}$$

$$\frac{df_6}{d\eta}(f_3-\eta f_1)-2f_1f_6-\frac{2D(\eta)}{(\gamma'_c/\Gamma_c)^2}\left(\frac{df_4}{d\eta}\right)^2-\frac{1}{\eta}\frac{d}{d\eta}\left(\eta\frac{B(\eta)}{\sigma_\gamma^2}\frac{df_6}{d\eta}\right)+Gf_6=0$$

$$\bar{\gamma}^2 \text{ Eq.} \tag{11d}$$

where $B(\eta)=\nu_T/\{U_{x,c}(x-a)\}$, $D(\eta)=D_T/\{U_{x,c}(x-a)\}$

and $G=12D_m/\{\varepsilon^2U_{x,c}(x-a)\}$.

Therefore, the self-preserving solutions $f_1\sim f_6$ for a circular jet are obtained by solving the ordinary differential equations (11a, b, c, d) with parameters B, D(or S_{cT}),σ_γ^2 and γ_c'/Γ_c. Generally, B, D and σ_γ^2 are functions of variable η and γ_c'/Γ_c is a function of variable ξ. Concerning $f_6(\eta)$, we have the following boundary conditions $f_6(0)=1$, $\lim_{\eta\to\infty}f_6(\eta)=0$ and the value of parameter G should be selected to satisfy these conditions.

4. 2. Calculation results and discussion

In order to investigate the effects of parameters B, D(or S_{cT}) and σ_γ^2 on the self-preserving function $f_6(\eta)$, firstly in the case where all of B, D(or S_{cT}), σ_γ^2

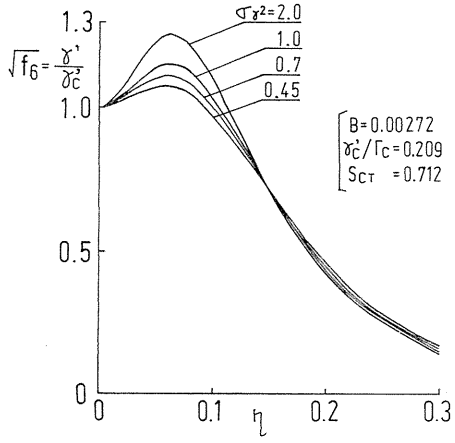

Fig. 10. The effect of parameter σ_{γ^2} on the self-preserving solution $\sqrt{f_6}$.

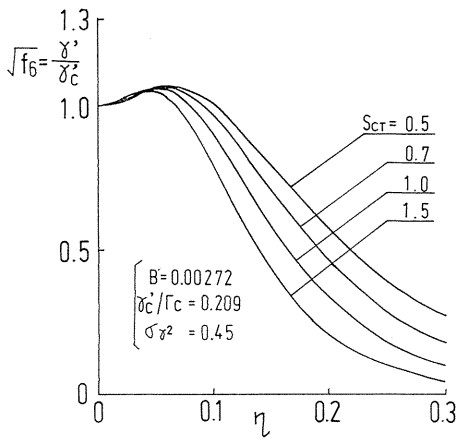

Fig. 11. The effect of parameter S_{CT} on the self-preserving solution $\sqrt{f_6}$.

and γ_C'/Γ_C are assumed to be constant in a self-preserving field, the solutions for $f_6(\eta)$ have been calculated.

In Fig. 10, the effects of parameter σ_{γ^2} on $\gamma'/\gamma_C'=\sqrt{f_6}$ are investigated, where $B=0.00272$ (Fig. 5), $S_{CT}=0.712$ (Fig. 7) and $\gamma_C'/\Gamma_C=0.209$ (Fig. 9) are used from the present experimental results. From this figure, it is found that parameter σ_{γ^2} has a large infuluence on a peak value of the γ'/γ_C' profile, that is, the peak values tend to increase as the increase of σ_{γ^2} value.

In Fig. 11, the effect of parameter $S_{CT}=\nu_T/D_T$ on γ'/γ_C' profiles is investigated, where $\sigma_{\gamma^2}=0.45$ and the values of B, γ_C'/Γ_C are the same as mentioned above. As shown in Fig. 11, the width of γ'/γ_C' profiles tends to decrease remarkably as S_{CT} increases. However, it should be noticed that the values of S_{CT} over 1.0 mean that the mean concentration profiles have narrower width than that of the mean velocity profiles and these phenomena are inconsistent with the experimental results. Judging from the calculated results in Fig. 10 and Fig. 11, we can see that the solutions obtained have the same tendency as a present experimental similar profile qualitatively but there appears an appreciable difference between experimental results and the calculated self-preserving solutions. As the cause of this difference it can be considered that the constancy of ν_T, D_T, the assumption of the gradient type diffusion process for the three-order correlation (Eq. (8)) between the concentration and velocity fluctuation and the assumption of an isotropic scalar field for a dissipation term (Eq. (9)) are not good approximations in this case.

Firstly, in these assumptions the constancy of ν_T, D_T will be examined. When the radial profiles of U_x, Γ i.e. $f_1(\eta)$, $f_4(\eta)$ are approximated to the Gaussian profiles Eq. (1), Eq. (3) based on the experimental results in order to give the mean velocity and mean concentration field the more accurate informations, the γ'/γ_C' profile as well as radial profiles of ν_T, D_T can be calculated.

Fig. 12 shows the profiles of ν_T, D_T and in Fig. 13 a solid line denotes the $\gamma'/\gamma_C'=\sqrt{f_6}$ profile calculated by using above ν_T, D_T profiles, where S_{CT}, σ_{γ^2} and γ_C'/Γ_C are taken to be constant as $S_{CT}=0.712$, $\sigma_{\gamma^2}=0.7$[13,14] and $\gamma_C'/\Gamma_C=0.209$ respectively. In Fig. 13, a chain line is a similar profile obtained from the experimental results in $x/d_N\geq 100$. As shown in Fig. 12, ν_T and D_T have a tendency to

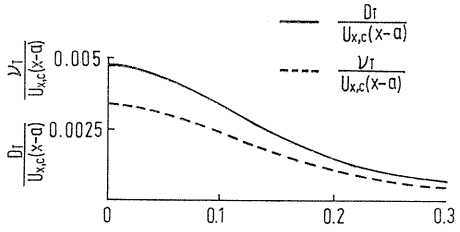

Fig. 12. The radial profiles of ν_T, D_T computed from the Gaussian function.

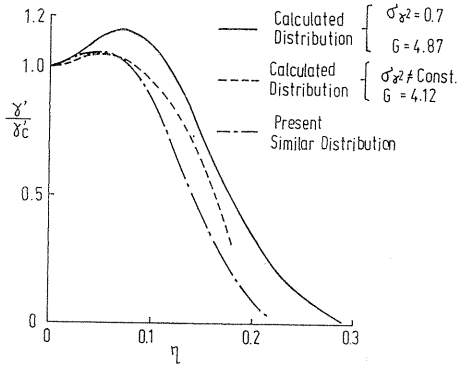

Fig. 13. The comparative diagram between the self-preserving solutions and the experimental similar profile.

decrease as the increase of variable η so the constancy of ν_T and D_T in a flow field is not appropriate. Although the calculated γ'/γ_C' profile (a solid line) shown in Fig. 13 has a bigger peak value and a larger width as a whole than a present experimental similar profile (a chain line), the shapes of those two profiles are almost consistent with each other so we can say that a fairy improved profile in comparison with ones calculated by using the condition of constant ν_T and D_T has been obtained. However, these still appears a deviation between calculated profiles and measured values so as mentioned ealier, the examinations for the assumption of gradient type diffusion process for the three-order correlation between the

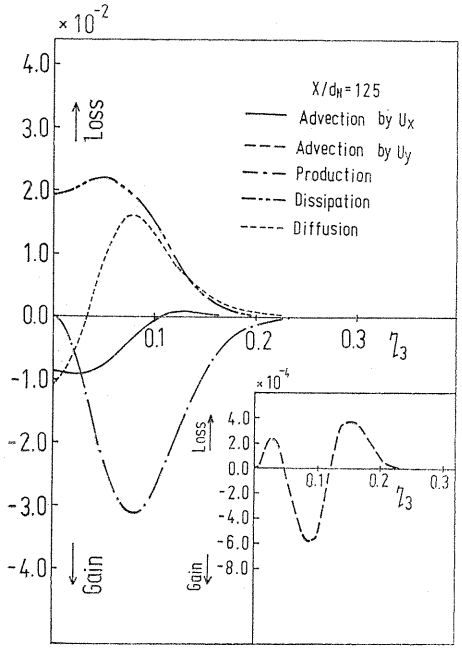

Fig. 14. The balance of the concentration fluctuation intensity $\overline{\gamma}^2$ equation.

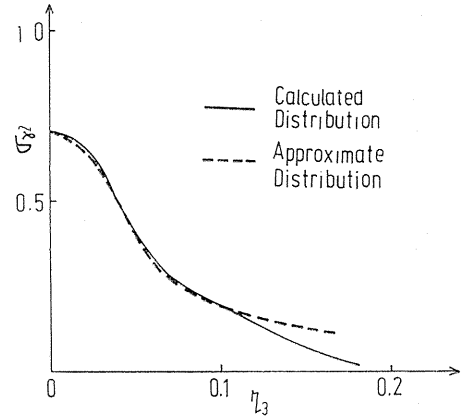

Fig. 15. The radial profiles of σ_{γ^2}.

concentration and velocity fluctuation (Eq. (8)) and the assumption of an isotropic scalar field for a dissipation term (Eq. (9)) are necessary. Now, in order to examine the propriety of the gradient type diffusion model (Eq. (8)), each term of the $\overline{\gamma}^2$ equation (Eq. (5d)) is calculated on the basis of the experimental results and the profile of $\sigma_\gamma{}^2$ is predicted from a shape of a diffusion term. Fig. 14 shows the balance of Eq. (5d) which is rewritten in a non-dimensional form by using Γ_C, $U_{x,c}$ and b_Γ where the dissipation term is estimated by using the assumption of an isotropic field (Eq. (9)). It is noticed here that the diffusion term is determined by adjusting the magnitude of dissipation term in order to keep the continuity of the $\sigma_\gamma{}^2$ profile for variable η, hence the general requirement to the diffusion term i. e. $\int_0^\infty r\times(\text{diffusion term})dr\equiv 0$ is not satisfied. In Fig. 15, shown is the $\sigma_\gamma{}^2$ profile (a solid line) calculated from the diffusion term in a way mentioned above. From this figure, it can be seen that the $\sigma_\gamma{}^2$ profile has a notable change in a jet flow field so the constancy of $\sigma_\gamma{}^2$ is not satisfied. Hereupon, when the $\sigma_\gamma{}^2$ profile is approximated to a broken line in Fig. 15 and the self-preserving solution $\gamma'/\gamma_C'=\sqrt{f_6}$ is again calculated, we can get the broken line shown in Fig. 13. Although this profile is pretty close to an experimental similar profile, the boundary condition of $\lim_{\eta\to\infty} f_6(\eta)=0$ is not satisfied.

5. Conclusions

In the circular free jet into a quiescent water, the mean velocity field, mean concentration field and fluctuating concentration field were measured. The experimental results are as follows.

(1) The radial profiles of the mean velocity and mean concentration have similar shapes in the extent $30\leq x/d_N\leq 200$, $50\leq x/d_N\leq 175$ respectively and they are approximated well to Gaussian profiles Eq. (1), Eq. (3).

(2) The radial profiles of the concentration fluctuation r.m.s. value γ' become similar only in the pretty downstream extent $x/d_N\geq 100$.

On the basis of above experimental results, with regard to the radial profile of the concentration fluctuation intensity the self-preserving solutions are calculated by using the assumptions of the gradient type diffusion process and those properties are investigated. The obtained results are as follows.

(3) Although the self-preserving solutions which are calculated by using the gradient type diffusion model in consideration of a change of the $\sigma_\gamma{}^2$ value are qualitatively consistent with the present experimental similar profile, those solutions are still insufficient to describe concentration field accurately, hence hereafter the more detail examinations will be required together with the improvement of the measuring accuracy for γ'.

References

1) Lee, J. and Brodkey, R. S., *Rev. Sci. Instrum.*, Vol. 34, No. 10 (1963), pp. 1086-1090.
2) Nye, J. O. and Brodkey, R. S., *Rev. Sci. Instrum.*, Vol. 38, No. 1 (1967), pp. 26-28.
3) Nakamura, I., Miyata, M. and Sakai, Y., *Preprint of JSME*, No. 813-2 (1981-3), pp. 15-

17, in Japanese.
4) Becker, H. A., Hottel, H. C. and Williams, G. C., *J. Fluid Mech.*, Vol. 30, part 2 (1967), pp. 285–303.
5) Birch, A. D., Brown, D. R. and Thomas, J. R., *J. Fluid Mech.*, Vol. 88, part 3 (1978), pp. 431–449.
6) Shiragashi, M. and Tomita, Y., *Trans. JSME*, Vol. 43, No. 375 (1978–11), pp. 4186–4194, in Japanese.
7) Corrsin, S. and Uberoi, M. S., *NACA*, TN., No. 1865 (1949).
8) Wilson, R. A. M. and Dankwerts, P. V., *Chem. Eng. Sci.*, Vol. 19 (1964), pp. 885–895.
9) Spalding, D. B., *Chem. Eng., Sci.* Vol. 26 (1971), pp. 95–107.
10) Hinze, J. O., *Turbulence*, 2nd ed., McGrall-Hill, (1975), p. 288.
11) Friehe, C. A., Van Atta, C. W. and Gibson, C. H., *in Turbulent Shear Flows, AGARD Conference Proceedings* No. 93 (1972), p. 18–1.
12) Antonia, R. A., Satyaprakash, B. R. and Hussain, A. K. M. K., *Phys. Fluids*, Vol. 23, No. 4(1980), pp. 695–700.
13) Sutton, G. W., *AIAA Journal*, Vol. 7, No. 1 (1969), pp. 90–95.
14) Meshcheryakov, YE. A., *Fluids Mechanics—Soviet Research*, Vol. 5, No. 4(1976), pp. 54–62.